Composites Part A 132 (2020) 105821

Contents lists available at ScienceDirect

Composites Part A

journal homepage: www.elsevier.com/locate/compositesa

Use of computed tomography to determine penetration paths and the distribution of melamine resin in thermally-modified beech veneers after plasma treatment

Richard Wascher[a,b], Florian Bittner[c,d,*], Georg Avramidis[a], Martin Bellmann[a], Hans-Josef Endres[c,d], Holger Militz[b], Wolfgang Viöl[a]

[a] University of Applied Sciences and Arts, Faculty of Natural Sciences and Technology, Von-Ossietzky-Strasse 99, 37085 Göttingen, Germany
[b] Georg-August-University of Göttingen, Wood Biology and Wood Products, Büsgenweg 4, 37077 Göttingen, Germany
[c] Fraunhofer Institute for Wood Research, Wilhelm-Klauditz-Institut WKI, Heisterbergallee 10A, 30453 Hannover, Germany
[d] Leibniz University Hannover, Institute of Plastics and Circular Economy IKK, An der Universität 2, 30823 Garbsen, Germany

ARTICLE INFO

Keywords:
D. CT analysis
E. Heat treatment
E. Resin flow
E. Surface treatments

ABSTRACT

In this study, X-ray computed tomography was used to detect flow paths and the distribution of melamine resin in thermally-modified and subsequently plasma-treated beech veneers. By introducing iodide as a contrast agent, the melamine resin deposition in veneer samples could be visualized and quantified. The investigations showed that the deposition of melamine resin within the lumina and cell walls of the reference samples was limited to near-surface areas. In contrast to the reference, the plasma-treated samples showed a higher loading with the modifier, both in the near surface and in the deeper areas of the sample. Increased resin infiltration was observed in the production-related micro-cracks only in the plasma-treated samples. Plasma-treated samples displayed a significant increase in impregnated volume compared to non-plasma-treated samples, both in the lumina and cell wall areas.

1. Introduction

The advantages of wood such as CO_2 neutrality, physical properties etc. are commonly known and mentioned in numerous scientific publications. However, especially in the construction-related use of common European wood species in outdoor areas, there is a decisive disadvantage, which significantly reduces the application portfolio of this material: the dimensional stability of wood is unsuitable due to its natural swelling and shrinkage behavior. Usual measures to deal with this issue include protective structural solutions or sealing the surfaces with appropriate coatings, which can be complex and time-consuming or have only a limited durability. In the last decades, there has been a rapid development of scientifically elaborated methods to increase the dimensional stability of wood on the basis of a chemical or physico-chemical modification of the material (acytelation, furfurylation, thermal modification etc.), which has led to technological advances and the successful commercialization of some of these methods (e.g. Accoya, Keybony) [1]. The majority of these approaches are based on reducing or blocking of free OH-binding sites within the material, which prevents the reaction with water molecules and thus their incorporation into the wood fibrils, or on blocking the natural pathways for liquids in the wood [1–3]. Most of these applications - depending on the selected process parameters - result in reducing the swelling of the wood and thus in improving the dimensional stability. In the case of chemical modification of wood, an increase in dimensional stability is dependent on the degree of loading with the respective modification agents, especially on the mass of the modifiers deposited within the wood cell walls [4,5]. Simple immersion processes at atmospheric pressure either do not usually lead to sufficient loading of the material or require long process times. Vacuum-pressure impregnation processes are also time-consuming and require a relatively high expenditure on technical equipment, even though they represent a frequently used method to ensure extensive soaking and distribution of the modification agents within the wooden volume. However, the use of gas discharges (or plasmas) as part of the impregnation process allows the use of conventional dipping processes or roller applications for impregnation as long as thin materials such as veneers are used and no complete impregnation of the material is required [6,7]. This type of surface modification involves numerous physico-chemical interactions of plasma-generated reactive species with the wood surface, which may

* Corresponding author at: Leibniz University Hannover, Institute of Plastics and Circular Economy IKK, An der Universität 2, 30823 Garbsen, Germany.
E-mail address: bittner@ikk.uni-hannover.de (F. Bittner).

https://doi.org/10.1016/j.compositesa.2020.105821
Received 3 September 2019; Received in revised form 31 January 2020; Accepted 6 February 2020
Available online 07 February 2020

result in cleaning, ablation, crosslinking effects [8,9], and/or the generation of the requested functional groups on the treated material surface [10]. Plasma-based wood modification can be realized by using a gas discharge operated with oxygen-containing gases such as air, so that the material is provided with hydrophilic properties leading to positive effects on the subsequent process steps [11,12]. In recent years, several publications have reported a significantly improved uptake of modification agents of plasma pre-treated wood veneers [13–16]. Generally, plasma-based effects are limited to the outer surface layer. Král et al. indicate that the maximum penetration depth of a plasma discharge into the interior of the wood (*Fagus sylvatica*) can be up to approx. 300 nm [17]. In the case of the plasma treatment of beech veneers, however, Wascher et al. have demonstrated the known plasma effects at a depth of 0.9 mm (total thickness = 1.8 mm) [18]. The authors attribute these observations to the occurrence of gas discharges in the wood cavities (e.g. vessels, cracks), resulting in an accelerated inflow of liquid into the wood cavities. In this context, Wascher et al. [19] have demonstrated a higher bulking of plasma-treated beech veneers impregnated with DMDHEU compared to reference samples at equal solution uptake, whereas the comparable solution uptake of the reference samples required significantly longer immersion times. The authors therefore assume that a more homogeneous distribution of the modifier (here: DMDHEU) in the wood body can be promoted by plasma pretreatment compared to the reference. Furthermore, plywood samples made from thermally-modified, plasma-treated beech veneers and subsequently impregnated with melamine resin show a higher shear strength than the reference at comparable solution uptake (in this case, more than a hundredfold immersion times were necessary to achieve comparable values for solution absorption) [20]. These observations give rise to the assumption that the plasma pre-treatment of wood veneers can lead to differences in the distribution of modifiers within the sample. Since no direct verification of these differences in the distribution in the veneer volume exists yet, there is a need to detect the penetration or flow paths of the liquid in order to elucidate the plasma's mechanisms of action within the wood bulk. This requires a three-dimensional (3D) measurement method for quantifying the amount of modification agents introduced and for visualizing the flow profile of the liquid.

Various publications deal with spatially resolved investigations of depositing modification agents within the wood volume. Several of these studies focus on a detailed two-dimensional (2D) representation of modifier deposits within the wood cell at high resolution, considering single cell wall components. For instance, Gindl et al. determined the storage of melamine in the cell walls (secondary cell wall and middle lamella) of spruce using UV-microscopic methods and nano intendation techniques [21–23]. Rapp et al. [5] reported similar results using EELS (electron energy loss spectroscopy). They observed melamine resin deposits in the S2, S3 and middle lamella of spruce, with the melamine deposit in S2 — contrary to expectation — being the weakest. SEM/EDX methods provide very accurate information about the wood structure and the location of modification reagents such as siloxanes within the sample volume [24]. However, all the methods presented are limited to sample sections, which means that only high-resolution information can be obtained in 2D. That implies it is not readily possible to determine the distribution of the modifier in the entire sample volume, for example to identify penetration paths of the modifier into the core material.

In recent years, studies in this field of research have used X-ray computed tomography (CT) for the detection and 3D visualization of modifiers and adhesive systems in wood volume. As the micro-CT is a non-destructive method, it is possible to examine the same wood sample before and after impregnation with modification agents *in situ*. De Vetter et al. demonstrated the potential of this method on Scots pine and beech samples impregnated with siloxanes/silanes mixture (bromine was added to the modifier to enhance the contrast) [24]. McKinley et al. [25] investigated adhesive bonding on three different types of wood and with different adhesive systems, as well as the penetration behavior of the glue into the wood volume by use of micro-CT. However, due to the limited resolution of the CT-method, the depiction of the intracellular deposition of modifiers was supported by supplementary SEM/EDX measurements.

Therefore, the CT method aided by the application of a contrast agent to the resin solution can represent an adequate solution for the questions posed in this study. These questions primarily include the identification of penetration paths and the location of melamine resin in the wood structure of plasma-pretreated and untreated thermally-modified beech veneer. In addition, an approval and discussion of the load levels presented in previous studies by the authors will be conducted in the context of the current study.

2. Material and methods

2.1. Materials

Thermally-modified rotary-cut beech (*Fagus sylvatica*) veneers were purchased from OWI GmbH, Germany. The thermal modification of beech veneers was carried out at approx. 200 °C and a treatment time of 20 min [26]. Samples with the dimensions of approx. 29 × 7 × 1.2 mm^3 were stored at standard condition (20 °C and 65% RH) for 24 h, resulting in an equilibrium moisture content (EMC) of approximately 7.7% [16]. Melamine resin (Madurit MW 840, solid content 75%) was purchased from INEOS Group AG, Germany, and was mixed with a corresponding amount of potassium iodide (Carl Roth GmbH, Germany) to obtain iodine mass contents of 0, 1 or 5%, respectively.

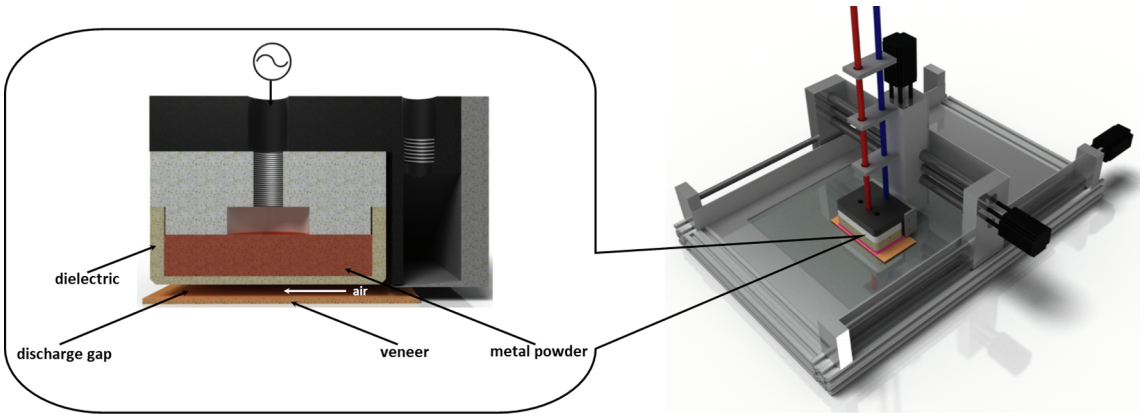

Fig. 1. Plasma setup. (For interpretation of the references to colour in this figure legend, the reader is referred to the web version of this article.)

2.2. Plasma setup

Plasma treatments were carried out with the ABO 20.1 plasma system developed at the University of Applied Sciences and Arts (Fig. 1). The plasma system is based on the principle of a dielectric barrier discharge (DBD) [27]. The system consists of a positioning unit with three degree of freedom and its effective treatment area is 410 × 330 mm^2 at speeds of up to 8000 mm/min. The positioning unit is controlled with the aid of software which can be used to set all the relevant treatment parameters (e.g. electrode-to-sample distance, treatment time, positioning speed, treatment areas and number of repetitions). Samples were placed on an aluminum plate with an embedded glass plate so that the aluminum/glass plate acts as a ground electrode. The electrode is mounted on the Z-axis mount. The electrode consists of a flat ground ceramic crucible (base thickness 3 mm) which serves as a dielectric barrier. The ceramic crucible is filled with a bronze powder. The electrode cover is made of PTFE. The electrode is integrated in a plastic housing, which has a gas supply (compressed air) and high-voltage connection as well as an air supply chamber. The distance between the high voltage electrode and the ground electrode was set to 5 mm. The high-voltage electrode was connected to a power supply which generated a pulsed voltage of approx. 31 kV (peak) with alternating polarity, and a pulse repetition frequency of 17 kHz. During plasma treatment, the power coupled into the discharge volume amounted to approx. 700 W and the treatment time was 5 s. A temperature of 60 °C was not exceeded during plasma treatment. More detailed information on this plasma system can be found in ten Bosch et al [28]. Peters et al. characterized a similar system considering rotational-, vibrational - and electron temperatures as well as reduced electrical field strength [29].

2.3. Melamine uptake

The melamine resin impregnation (with a solid content of the melamine resin of 50%) of the samples was carried out using an immersion test setup at atmospheric pressure and at a liquid temperature of 20 °C. The setup is entirely described in Wascher et al. [30] and allows automated measurements with high reproducibility. The samples were impregnated immediately after the plasma treatment. The reference samples were impregnated with melamine resin without prior plasma treatment. The residual liquid was removed from the veneer surface with a scraping device. The immersion time was 1 s.

2.4. Micro-CT measurements

CT is based on the collection of X-ray absorption images of a specimen from different rotational angles (Fig. 2 left). In the reconstruction process, a 3D volume is calculated from the X-ray images. It consists of voxels, whose edge length mainly defines the resolution of the measurement. The grey value of each voxel reflects the local X-ray absorption characteristic. A high grey value represents a high X-ray absorption. This representation enables one to distinguish different materials in the CT measurement.

The micro-CT measurements of the veneer samples were performed on a CT-AlphaDuo device (Procon X-Ray GmbH, Sarstedt, Germany). To maximize the scan resolution while capturing a large proportion of the samples, the microCT scans were performed in helix mode. In addition to the rotational movement known from standard micro-CT in helix CT the sample is shifted in the direction of the rotational axis. This method reduces Feldkamp artefacts and allows to measure samples with a high aspect ratio in a given resolution that exceed the detector size. A stitching of several scans would be required to achieve comparable results with standard micro-CT.

The parameters of the micro-CT measurements are given in Table 1. The preliminary scans were performed after the impregnation process to evaluate the effect of different iodine concentrations as contrast agent in the resin. The subsequent scans of the plasma-treated and non-plasma-treated samples were conducted before impregnation, after impregnation and – in case of non-plasma-treated sample 1 and plasma-treated sample 1 – again after the curing process. For visualization and analysis of the volume data, VGSTUDIO MAX 3.2 (Volume Graphics GmbH, Heidelberg, Germany) was used.

2.5. SEM-EDX

The samples for SEM-EDX analysis were prepared from a sliding microtome with single-use blades. The samples were provided with 20 µm gold sputter coating to avoid charging effects. The SEM images were acquired with an EVO LS 15 (Carl Zeiss Microscopy GmbH, Jena, Germany) using a 8.5 mm working distance, and a 10 kV acceleration voltage. The EDX images were recorded with an X-MAX 50 mm^2 detector (Oxford Instruments GmbH, Wiesbaden, Germany) in combination with the AzTecEnergy program, a recording time of 150 s and a scan size of 2048 × 1664 px. Nitrogen data were captured by elemental mapping and used for melamine resin distribution analysis.

3. Results and discussion

Previous publications have demonstrated a significantly improved liquid absorption of wood veneers after plasma treatment [14,15]. For instance, the water uptake of beech veneer can be increased — at an immersion time of 1 s — by up to 150% [13]. When impregnating

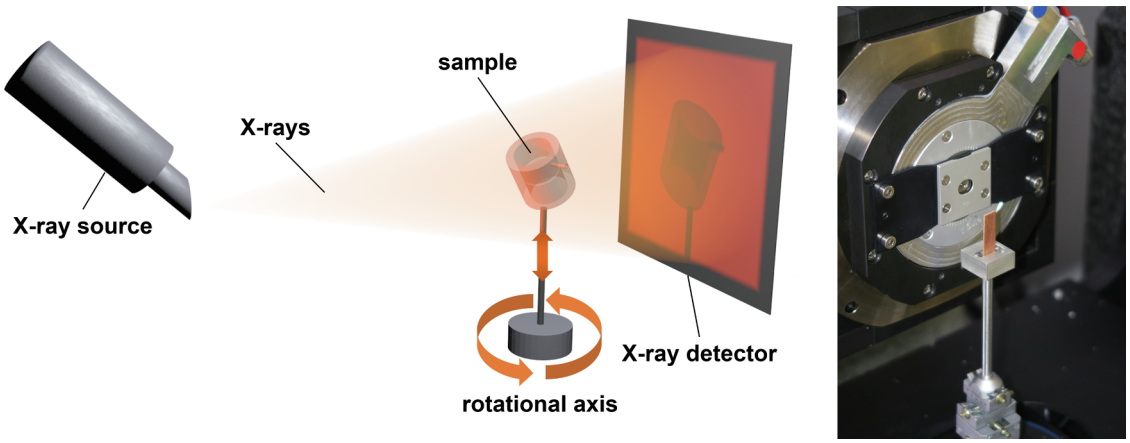

Fig. 2. Schematic CT measurement setup (left) and veneer sample positioned in front. (For interpretation of the references to colour in this figure legend, the reader is referred to the web version of this article.)

Table 1
micro-CT measurement parameters.

	Preliminary samples without plasma treatment	non-plasma-treated samples 1 & 2; plasma-treated samples 1 & 2
X-ray tube voltage/kV	60	60
X-ray tube current/µA	150	150
Focus-object-distance/mm	25	25
Focus-detector-distance/mm	600	600
No. of projections	1334	3760
Integration time/ms	6 × 400	6 × 400
Scan volume/mm^3	ca. 2.5 × 7 × 1.2	ca. 15 × 7 × 1.2
Voxel resolution/µm	5.7	5.7

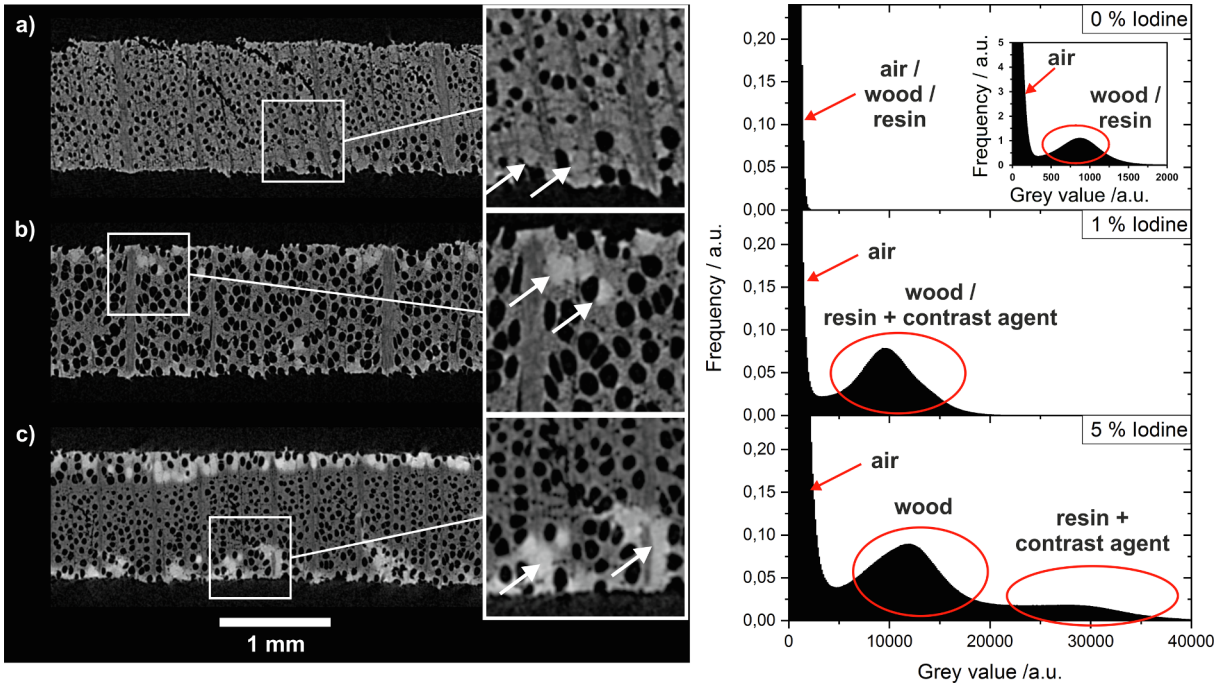

Fig. 3. Effect of iodine concentration in melamine resin on grey value distribution in microCT scans of impregnated veneer samples. White arrows indicate resin-filled lumina and resin-infiltrated cell walls. (a) Resin without contrast agent; (b) resin with 1% iodine; (c) resin with 5% iodine.

thermally-modified beech veneers with melamine resin, the solids content can be significantly increased at the same immersion time [16]. However, the determination of solid content of the modifier or weight percent gain (WPG) provides no information about the spatial distribution or location of the modifier within the sample volume.

In this study, micro-CT measurements of thermally-modified beech veneers impregnated with a 50% (m/m) melamine solution were initially conducted in order to differentiate the melamine resin from the wood components by contrast differences. Fig. 3a shows a micro-CT image of a veneer sample impregnated with melamine resin solution as purchased. However, there are no significant differences observable in the grey value between the wood tissue and the melamine resin. The grey value of the individual voxels of a micro-CT scan represents the local X-ray attenuation characteristic of the material and depends to a large extent on the mean atomic number [31]. Since both wood and melamine resin are predominantly based on low-attenuation elements like hydrogen, nitrogen, oxygen and carbon, they exhibit similar X-ray attenuation characteristics. In the present case, this leads to poor contrast and makes a separation by means of image segmentation of resin and wood difficult.

To enhance the contrast between similarly absorbing materials, contrast agents can be applied to increase the mean atomic number of one component [32–36]. In our study for this purpose, potassium iodide — due to the low water solubility of elementary iodine — was dissolved in the melamine resin before impregnation. Iodine concentrations of 1% and 5% were evaluated in a preliminary experiment with non-plasma treated samples to identify the iodine concentration required to distinguish wood and melamine resin.

Adding 1% iodine (corresponding to 1.3 mass percent potassium iodine) to the melamine solution led to a weakly enhanced contrast between the wood and the melamine resin (Fig. 3b). The histogram shows a fluent transition of grey values representing wood and iodine-loaded resin. While a qualitative, visible identification of resin inside the sample was possible, a quantitative separation by means of a threshold value was not possible.

At an iodine content of 5% (Fig. 3c), it is unambiguously possible to locate the introduced iodine-loaded melamine resin within the sample. The respective histogram shows two separate peaks for wood and iodine-loaded resin. Since the differences in contrast were considered sufficient for an addition of 5% iodine to the melamine solution, this setting was retained for all subsequent experiments.

The authors are aware that the addition of the contrast agent potassium iodide to the melamine solution could change the viscosity as well as the polarity of the solution. This can affect the infiltration behavior of the solution. In contrast to other studies on the infiltration behavior of resin, the contrast agent was not chemically bonded to the resin. Therefore, it cannot be excluded that a separation of potassium iodide and resin solution may take place during the infiltration process, implying a migration of contrast agent into the wood tissue [36,37]. For the comparison of the infiltration behavior of non-treated and plasma-

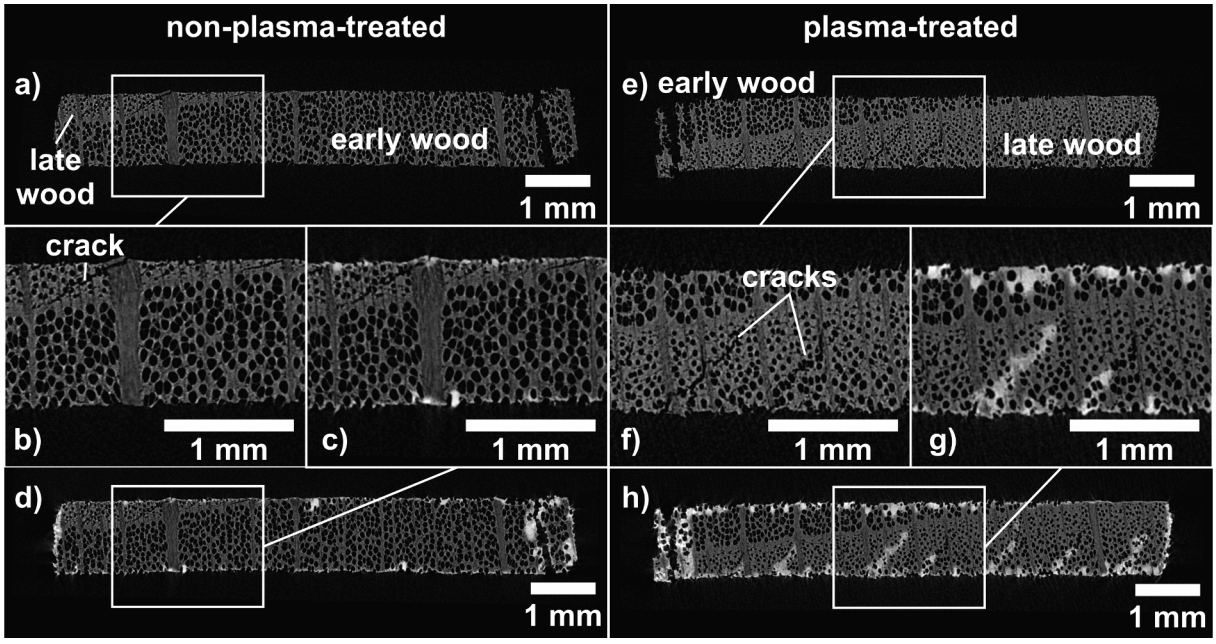

Fig. 4. microCT cross sections of (a and b) reference sample before impregnation; (c and d) reference sample after impregnation; (e and f) plasma-treated sample before impregnation; (g and h) plasma-treated sample after impregnation. (For interpretation of the references to colour in this figure legend, the reader is referred to the web version of this article.)

treated veneer samples, however, the influence of the contrast agent on the infiltration behavior appears negligible because it affects all samples to the same extent.

As already discussed, a major advantage of the micro-CT method is found in the non-destructive examination, which means that the micro-CT measurement has no influence on subsequent treatment steps within the scope of this work. Due to these method-specific properties, samples can be measured before and after impregnation with melamine resin (with and without plasma pretreatment) in order to detect the flow paths and the distribution of modification agents within the same sample. For this purpose, four samples were at first measured in the initial state and subsequently impregnated for 1 s with melamine resin, whereby two of the samples were additionally plasma-treated for 5 s before impregnation. Afterwards, a second micro-CT scan of each sample was performed.

Fig. 4 depicts the non-plasma-treated and plasma-treated samples before and after resin impregnation by representative micro-CT cross sections, (further cross sections can be found in the supplementary materials). Since wood is a natural product, differences between individual specimens are within expectation, but have to be considered for the evaluation of the measurement results. Differences in the wood anatomy of the analyzed veneer samples are apparent in Fig. 4a and e. While the reference samples consist mainly of early-wood, the plasma-treated samples contain early-wood as well as late-wood in similar proportions. Typical for rotary-cut veneers are the one-sided production-related cracks [38]. Cracks of the investigated samples seem to be limited to the late-wood, while early-wood parts of all samples revealed no cracks. Measurements showed no differences between plasma-treated samples and the reference with regard to the gap widths of the cracks (approx. 20 µm).

For the reference sample, a penetration of the melamine resin solution is apparently restricted to the near-surface areas (Fig. 4c and d) after an impregnation time of 1 s. The cracks present in the late-wood parts of these samples show no penetration of the modifier after impregnation (Fig. 4b and c). In contrast, samples treated with air-plasma prior to impregnation exhibited a considerably deeper penetration of the melamine resin into the veneer (Fig. 4g and h). However, not only an improved penetration of the melamine resin via the anatomically intact wood structures can be observed, but also the transport of the melamine resin into the bulk of the veneer is preferably promoted by the cracks (Fig. 4f and g).

These observations were supported by SEM/EDX analysis. Since nitrogen is an important structural component of melamine resins and this element only occurs in traces (< 1% [39]) in wood, an EDX analysis was performed on samples impregnated with pure melamine resin solution (with a solid content of the melamine resin of 50%) to create an elemental map of nitrogen as a marker for melamine resin.

Fig. 5a shows an SEM survey image (50× magnification) of the cross-section of a non-plasma-treated veneer sample. No lumina completely filled with melamine resin can be observed in the SEM overview. An EDX mapping was carried out (Fig. 5b); only in the areas near the surface of the sample do some lumen areas seem to be filled with melamine resin. Significant accumulations of nitrogen signals (conterminous melamine resin) can be observed mainly in the near-surface area. Nitrogen artefacts spread over the image section might be attributed to contamination of the sample during cutting by microtome.

In contrast, the plasma-pre-treated sample showed melamine resin deposits both in the near-surface areas and in the subjacent areas of the sample (Fig. 6a–e). Both SEM analysis and EDX-based elemental mapping show that some lumina located in the interior of the veneer are completely filled with melamine resin, and the cell walls of some vessels within the bulk show traces of modifiers (Fig. 6d and e). Furthermore, the SEM analysis shows that the imaged area of the plasma-treated sample does not display any visible cracks (compare with Fig. 4). Although the production-related cracks promote resin infiltration of the modifier in the plasma-treated samples, other ways of deeper penetration of the melamine resin into the bulk material are also conceivable (e.g. plasma-induced increased capillary action of the vessel elements [18]).

To visualize the penetration behavior of melamine resin for a representative sample size, a maximum intensity projection was used to image an overlay of a stack of micro-CT cross sections, representing the highest grey values present in the image stack (Figs. 7 and S5). In doing so, a sample height of 10 mm was condensed to one image. The impregnation depth of melamine resin inside the samples is highlighted this way. Neglecting the cutting edges of the sample, where resin

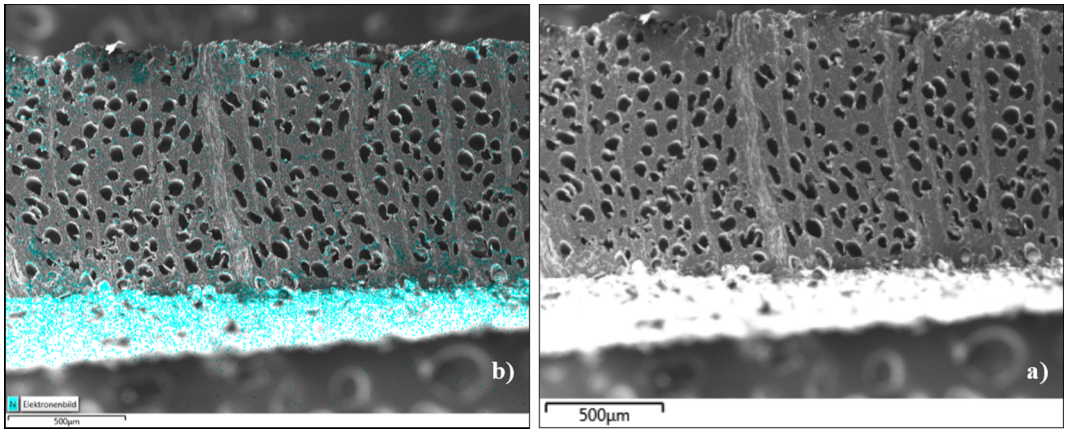

Fig. 5. SEM cross section of a reference sample after impregnation (50×) (a) and (b) represents EDX mapping of section (a). (For interpretation of the references to colour in this figure legend, the reader is referred to the web version of this article.)

impregnation is promoted, the reference sample in Fig. 7a shows a low impregnation depth with the bulk of the sample being almost resin-free. For plasma-treated samples, in contrast, the melamine resin solution penetrates deep into the bulk of the sample. A considerable amount of the modifier penetrates through the production-related cracks (see also Fig. 4). However, for the plasma-treated samples, the increased penetration of the modifier via the intact wood structures also seems to occur (see also Fig. 6). To support this observation, the penetration depths of the modifier were measured using the software for length provision in digital images "Datinf Measure" (DatInf GmbH, Germany, Version 3.0) in the early-wood areas ($n = 60$) located on the respective crack-free sides based on the micro-CT images. The mean value of the penetration depth for the non-plasma-treated sample (Fig. 7a) is approx. 160 µm (sd ± 30 µm) and thus differs significantly (two sample *t*-test, significance = 0.05) from the value of the plasma-treated sample (Fig. 7b) with a mean penetration depth of approx. 200 µm (sd ± 40 µm). The presented results corroborate the hypothesis of Wascher et al. [18], who suggests the occurrence of gas discharges within the cavities (cracks, lumina etc.) of wood veneers, provided the sample is located within the discharge volume (of at least a DBD).

To further investigate the variables that cause increased WPG of the plasma-treated samples, a detailed 3D analysis of impregnation volumes was performed. For this purpose, the following procedure was applied (Fig. 8): A surface determination based on a locally adaptive thresholding algorithm of the micro-CT scans of the samples before impregnation yielded a region of interest (ROI) describing the wood fraction (step 1). The scans of the samples after impregnation were aligned to the previous scans. By setting a threshold grey value, an ROI was created, covering material with increased grey value caused by resin impregnation (step 2). This ROI "impregnated material" includes pores filled with resin as well as resin-impregnated cell walls material. To differentiate pores and impregnated cell walls, two operations were performed. To obtain the ROI "impregnated wood", the intersection of the ROI "wood" and the ROI "impregnated material" was determined (step 3). The ROI of resin-filled lumina results from subtracting of the ROI "wood" from the ROI "impregnated material" (step 4). The ROI creation allows a visualization of the 3-dimensional distribution of resin-impregnated cell walls and resin-filled lumina as well as a quantitative analysis of the occupied volumes inside the samples.

To exclude influences of resin infiltration via the cutting edges of the veneers, a central section of 10 mm × 5 mm × d (d = sample thickness, ~1.2 mm) of the samples was selected for analyzing of the impregnation volumes. It correlates to the volumes condensed to maximum intensity projections (cf. Figs. 7 and S5). To further investigate the impregnation behavior in relation to the wood anatomy, smaller subsections limited to early- and late-wood were additionally analyzed (Fig. S6). To compare the volumes of resin-filled lumina and impregnated cell walls material between the samples, the determined volumes were related to the veneer surface area of the respective analysis volume through which resin infiltration can occur.

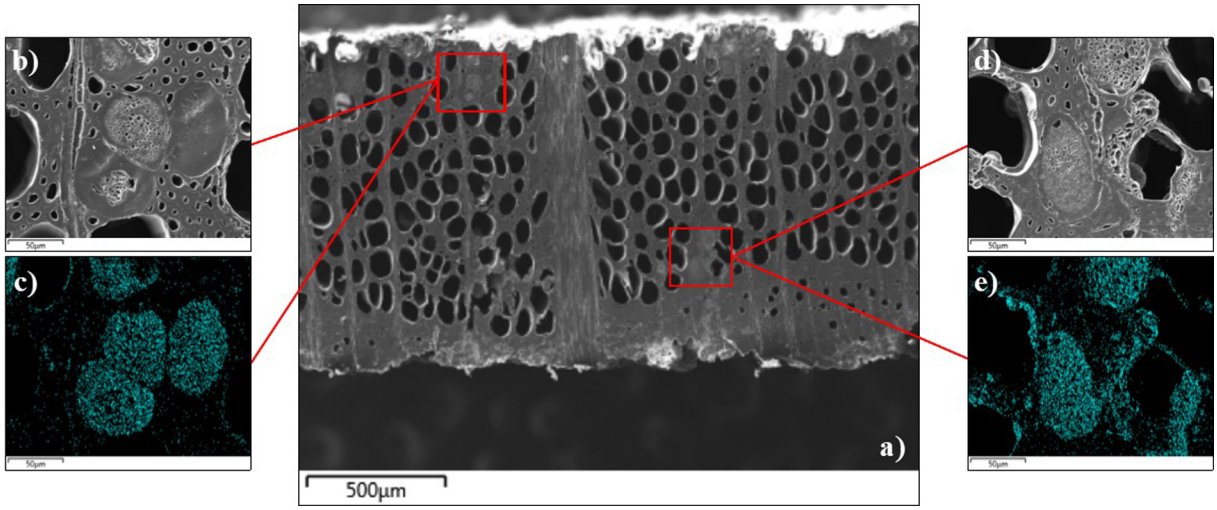

Fig. 6. SEM cross section of a plasma-treated sample after impregnation (50×) (a) and magnified sectors (500×) (b) and (d); (c) and (e) represent EDX mapping of section (b) and (d), respectively. (For interpretation of the references to colour in this figure legend, the reader is referred to the web version of this article.)

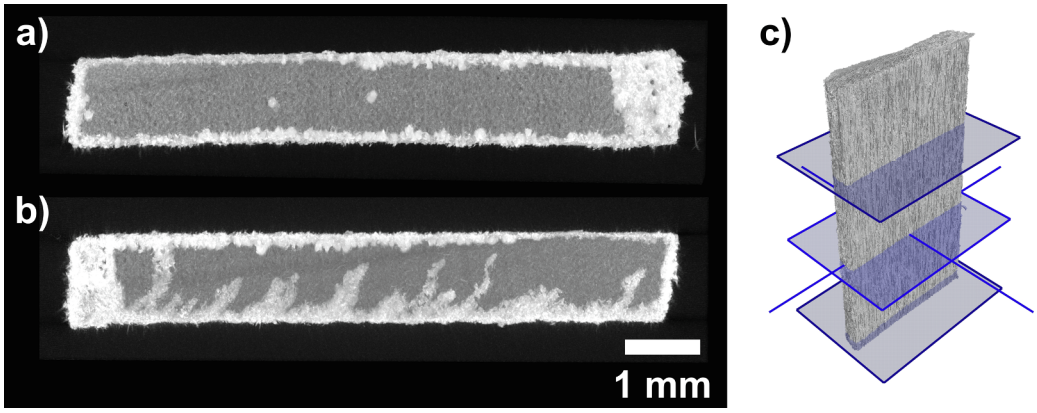

Fig. 7. Visualization of impregnation behavior by maximum intensity projections: Overlay of micro-CT cross sections over a sample height of 10 mm. (a) reference sample; (b) plasma-treated sample; (c) 3D image of non-plasma-treated sample. Top and bottom blue planes indicate the borders of the volume condensation. (For interpretation of the references to colour in this figure legend, the reader is referred to the web version of this article.)

The 3D view (Figs. 9 and S7) visualizes the deposition (and thus the flow paths) of the melamine resin introduced into the wood over the sections of analysis. As already shown in the 2D images of the samples, the melamine resin deposits of the reference samples are located mainly in the areas close to the surface (Figs. 9a and S7a). Analogously, the 3D visualization clearly shows an increased deposition of the resin along the cracks of the late-wood fractions in the plasma pre-treated samples (Figs. 9b and S7b).

Fig. 10 compares the surface-area-normalized impregnation volumes of the reference and plasma-treated samples. The amount of melamine resin introduced into the material in the plasma-treated samples was more than double in comparison to the references. However, plasma treatment does not lead to a significant change in the ratio between the modifier stored in the cell wall and the modifier remaining in the lumen.

The resin infiltration via cracks inside the late-wood fraction of the plasma-treated samples appears significant in comparison to the reference with minor late-wood fractions. This is confirmed by an increased impregnation ratio of the plasma-treated late-wood fractions in comparison to the early-wood fractions. The reference sample is not showing an increased impregnation in the late-wood fraction. This is consistent with the observation that the cracks in this sample are not filled with resin, leading to the hypothesis that plasma treatment promotes the resin impregnation via cracks, although the crack size is comparable to the crack size of the reference samples (see above). However, due to the small size of the late-wood fraction in only one of the two reference samples, the data basis is not yet sufficient to prove a generally different impregnation behavior of cracks. The early-wood fractions of the plasma-treated samples show also a significantly increased resin uptake in comparison to the early-wood fractions of the reference, proving that the increased uptake is not only related to the frequency and infiltration behavior of cracks. Instead, also the general resin infiltration capability is enhanced by plasma treatment. This differentiated evaluation of infiltration paths was possible only by a quantitative analysis of three-dimensional micro-CT data — an example of the diverse and powerful applications of micro-CT in material science.

It has to be noted that absolute values generated by the micro-CT method have a measurement uncertainty resulting among other things from the manually-adjusted threshold grey values for the resin-impregnated areas and the neglected effect of the contrast agent on resin viscosity and migration into wood tissue. For a comparison of the non-plasma-treated and plasma-treated samples, the method nevertheless appears valid to analyze the infiltration kinetics and to improve process parameters of plasma modification processes. The differences in impregnation volumes between reference and plasma-treated samples observed here, which are in the magnitude of at least two-fold increase, clearly exceed the measurement uncertainties of the micro-CT

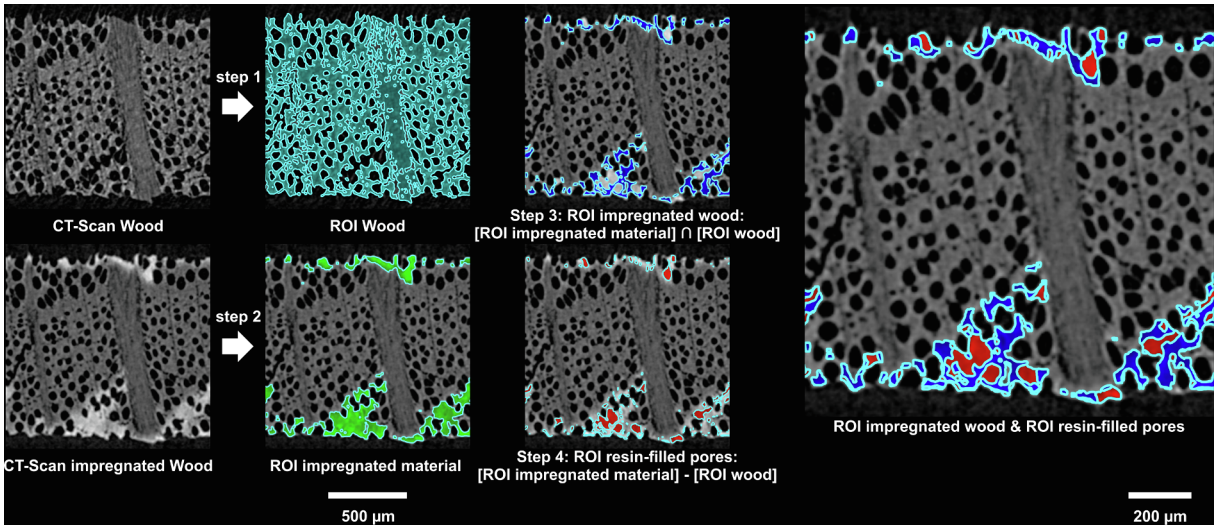

Fig. 8. Procedure for determination of impregnated cell walls and lumina volume. (For interpretation of the references to colour in this figure legend, the reader is referred to the web version of this article.)

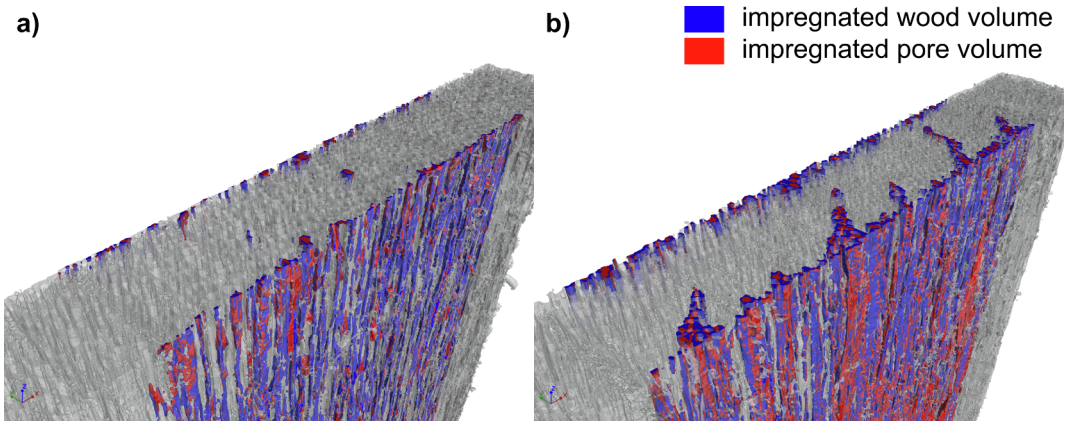

Fig. 9. 3D visualization of resin distribution in veneer samples. (a) Reference sample; (b) plasma-treated sample.

measurement as described here. As an indication for this estimate measurements of samples before and after curing, which will be described below, can be adduced. As expected, the comparison of these measurements results in very similar resin volumes for the same sample.

For future studies, especially of longer immersion times, however, the chemical bonding of a contrast agent to the resin, as described in literature [36,37], would be preferable to exclude especially the potential effect of contrast agent migration into the wood tissue.

A juxtaposition of the increase in the impregnation volume (reference/plasma-treated) in this study with the increase in the WPG (untreated/plasma-treated) from the previous studies (same material and comparable treatment conditions) [16] yields similar ratios. Thus, the increase in the WPG of thermally-treated beech veneers was approx. 130% [16]. The increase in impregnation volume determined by micro-CT in this study was strongly dependent on wood anatomy. While the overall increase was approx. 180%, the early wood fractions showed an increase of approx. 100% and the late wood fractions of 490%.

The last step of wood modification with melamine resins consists of a curing process. This process is generally associated with significant weight loss (polycondensation and water loss). In order to investigate whether this process is associated with morphological changes in the sample, two of the four samples (see Fig. 4) were stored for 60 min at 130 °C in an oven to polymerize the melamine resin. After the curing process, the samples were again examined by micro-CT. An exemplary comparison of the samples before and after the curing process initially shows only minor changes in morphology. The crystallization of the modifier partly creates cavities in the resin (shrink hole), which indicates a shrinkage of the resin (Fig. 11). The reference sample shows a comparable behavior as the plasma-treated sample shown in Fig. 11.

The quantitative analysis of the impregnated volumes before and after the curing process reveals only a minor decrease, which on one hand is consistent with the observed resin shrinkage, but on the other hand is not significant, considering the method's assumed measurement uncertainty (Fig. 12).

In summary, the results presented show a solid correlation to previous studies regarding melamine resin uptake and dimensional stability. Thus Wascher et al. [16] showed an accelerated melamine resin uptake and improved dimensional stability of plasma pre-treated thermally-modified beech veneers (same immersion time) in comparison to the reference samples. In a further study, plywood was produced from the plasma pre-treated veneers and reference veneers impregnated with melamine resin, whereby only the melamine resin introduced into the veneer during impregnation acted as adhesive (no additional adhesive in the adhesive joint) [20]. The WPG values of the reference veneers were approximately the same (with correspondingly longer immersion times) as those of the plasma pre-treated veneers. The results show an enhanced bonding quality despite the almost identical solids content of the modifier. If one also considers the results from Wascher et al. [19], which reported higher bulking during DMDHEU impregnation of beech veneers after plasma pretreatment, these results led to the assumption that plasma pretreatment of veneers results in better distribution or deeper penetration of modifiers in the samples. This hypothesis was corroborated by the present study.

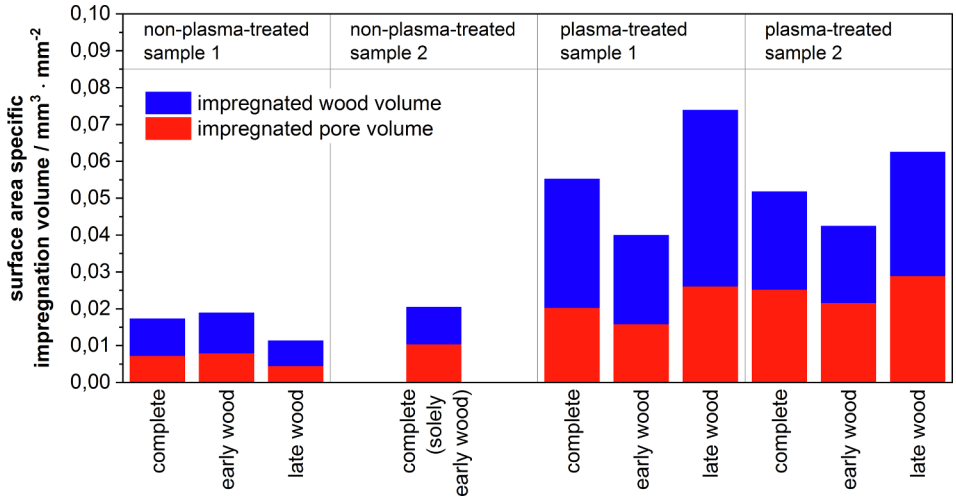

Fig. 10. Influence of plasma treatment on impregnated sample volumes. (For interpretation of the references to colour in this figure legend, the reader is referred to the web version of this article.)

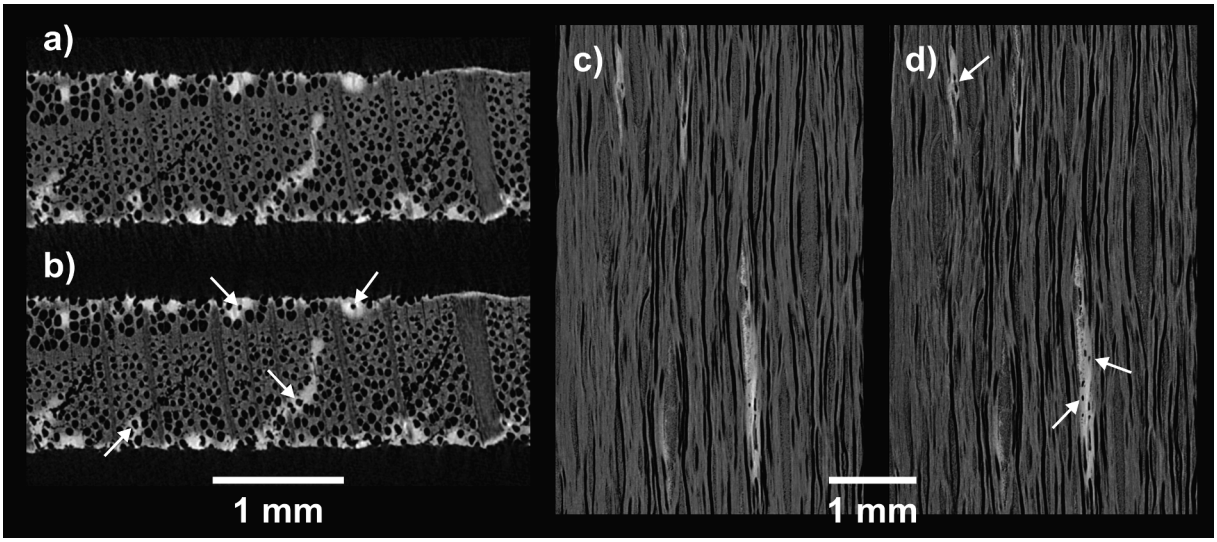

Fig. 11. Shrinkage of the resin in a plasma-treated sample as a consequence of the curing process. (a and c) Before curing; (b and d) after curing. Arrows indicate shrink holes.

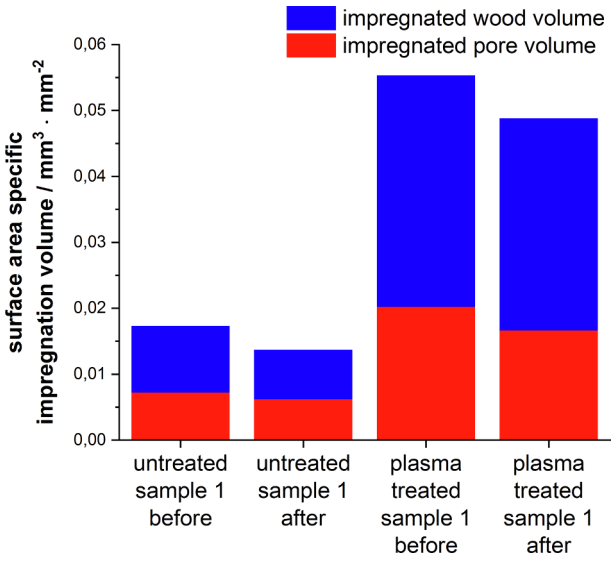

Fig. 12. Influence of curing process on impregnated volume. (For interpretation of the references to colour in this figure legend, the reader is referred to the web version of this article.)

4. Conclusion

Within the scope of this study, the suitability of the micro-CT method for the detection of flow paths and distribution of melamine resin within thermally-modified and subsequently plasma-treated beech veneers was successfully demonstrated. In conclusion it can be said that the micro-CT, despite its limited resolution e.g. in comparison to electron microscopy, is excellently suited for comparative measurements and process optimization. It turned out, that the use of a contrast agent in micro-CT measurements is essential to distinguish between melamine resin and wood structures. In the course of the investigations, it was demonstrated that the impregnation of lumina and cell walls with melamine resin in the samples not treated with plasma was limited to areas close to the surface. In contrast to the reference, the plasma-treated samples show a higher loading with the modifier both in the near surface and in the deeper areas of the veneer samples. These observations were additionally verified by SEM/EDX analysis. Increased resin infiltration could be observed in the micro-cracks of the plasma-treated samples. This effect could not be observed in the samples which were not treated with plasma. The micro-cracks, at least in the late-wood fractions, of the plasma-treated samples seem to promote resin infiltration. Plasma-treated samples show a significant increase in impregnated volume compared to non-plasma-treated samples with respect to melamine resin deposits both in the lumina and in the wood volume (cell wall areas). This applies to complete samples as well as to associated early-wood sections. The increase in melamine resin loading by plasma treatment for the early-wood fraction and the lack of resin infiltration via micro-cracks for the reference are in good agreement with the WPG measurements from previous studies. Further investigations on the behavior of the melamine resin deposits in the wood body after the curing process show a low formation of shrink holes in the resin. The general morphology and impregnated volumes do not change significantly.

Since it is already known that the quantity and penetration depth of the modification reagents to be introduced into the wood depend on the immersion time or plasma-specific parameters (e.g. treatment time, coupled power), a visualization of the impregnation process after longer immersion times is of interest. Furthermore, micro-CT represents a promising method to visualize the different penetration behavior of liquids (adhesives, modifiers, etc.) in early- and late-wood areas. Therefore, further studies on these topics are targeted.

CRediT authorship contribution statement

Richard Wascher: Conceptualization, Methodology, Validation, Formal analysis, Investigation, Writing - original draft, Writing - review & editing, Visualization, Supervision, Project administration. **Florian Bittner:** Conceptualization, Methodology, Validation, Formal analysis, Investigation, Writing - original draft, Writing - review & editing, Visualization, Supervision, Project administration. **Georg Avramidis:** Conceptualization, Methodology, Validation, Formal analysis, Investigation, Writing - original draft, Writing - review & editing, Visualization, Supervision, Project administration. **Martin Bellmann:** Conceptualization, Formal analysis, Writing - original draft, Visualization. **Hans-Josef Endres:** Resources, Supervision, Funding acquisition, Writing - review & editing. **Holger Militz:** Resources, Supervision, Writing - review & editing. **Wolfgang Viöl:** Resources, Funding acquisition, Supervision, Writing - review & editing.

Declaration of Competing Interest

The authors declare that they have no known competing financial interests or personal relationships that could have appeared to influence the work reported in this paper.

Acknowledgements

This work was supported by the Ministry of Science and Culture of Lower Saxony [grant number VWZN3102]; and the German Federal Ministry of Education [grant number 03XP0015B]. The authors would like to thank Dr. Roger Skarsten from the HAWK for proofreading and Tim Koddenberg from the University of Göttingen for valuable contentual input to the manuscript.

Appendix A. Supplementary material

Supplementary data to this article can be found online at https://doi.org/10.1016/j.compositesa.2020.105821.

References

[1] Hill CAS. Wood Modification: Chemical, Thermal and Other Processes. John Wiley & Sons; 2007.
[2] Ramage MH, Burridge H, Busse-Wicher M, Fereday G, Reynolds T, Shah DU, et al. The wood from the trees: The use of timber in construction. Renew Sustain Energy Rev 2017;68:333–59.
[3] Gérardin P. New alternatives for wood preservation based on thermal and chemical modification of wood— a review. Ann For Sci 2016;73:559–70.
[4] Hill CAS, Jones D. The dimensional stabilisation of corsican pine sapwood by reaction with carboxylic acid anhydrides. The effect of chain length. Holzforschung 1996;50:457–62.
[5] Rapp AO, Bestgen H, Adam W, Peek RD. Electron Energy Loss Spectroscopy (EELS) for quantification of cell-wall penetration of a melamine resin. Holzforschung 1999;53:111–7.
[6] Mai C, Verma P, Xie Y, Dyckmans J, Militz H. Mode of action of DMDHEU treatment against wood decay by white and brown rot fungi. In: Proceedings of European conference on wood modification. Stockholm, April; 2009. p. 45–52.
[7] Rowell RM. Handbook of Wood Chemistry and Wood Composites. CRC PressINC; 2012.
[8] Kogelschatz U, Eliasson B, Egli W. Dielectric-barrier discharges. Principle and applications. J Phys IV 1997;7:47–66.
[9] Kogelschatz U, Eliasson B, Egli W. From ozone generators to flat television screens: history and future potential of dielectric-barrier discharges. Pure Appl Chem 1999;71:1819–28.
[10] Klarhofer L, Viol W, Maus-Friedrichs W. Electron spectroscopy on plasma treated lignin and cellulose. Holzforschung 2010;64:331–6.
[11] Riedl B, Angel C, Prégent J, Blanchet P, Stafford L. Effect of wood surface modification by atmospheric-pressure plasma on waterborne coating adhesion. BioResources 2014;9:4908–23.
[12] Wolkenhauer A, Avramidis G, Militz H, Viöl W. Wood modification by atmospheric pressure plasma treatment. In: Proceedings of European conference on wood modification. Cardiff, October; 2007. p. 271–4.
[13] Avramidis G, Tebbe B, Nothnick E, Militz H, Viöl W, Wolkenhauer A. Wood veneer modification by atmospheric pressure plasma treatment for improved absorption characteristics. In: Proceedings of European conference on wood modification. Riga, September; 2010. p. 365–72.
[14] Avramidis G, Militz H, Avar I, Viöl W, Wolkenhauer A. Improved absorption characteristics of thermally modified beech veneer produced by plasma treatment. Eur J Wood Prod 2012;70:545–9.
[15] Wascher R, Schulze N, Avramidis G, Militz H, Viöl W. Increasing the water uptake of wood veneers through plasma treatment at atmospheric pressure. Eur J Wood Prod 2014;72:685–7.
[16] Wascher R, Kühn C, Avramidis G, Bicke S, Militz H, Ohms G, et al. Plywood made from plasma-treated veneers: melamine uptake, dimensional stability, and mechanical properties. J Wood Sci 2017;63:338–49.
[17] Král P, Ráhel' J, Stupavská M, Šrajer J, Klímek P, Mishra PK, et al. XPS depth profile of plasma-activated surface of beech wood (Fagus sylvatica) and its impact on polyvinyl acetate tensile shear bond strength. Wood Sci Technol 2015;49:319–30.
[18] Wascher R, Avramidis G, Vetter U, Damm R, Peters F, Militz H, et al. Plasma induced effects within the bulk material of wood veneers. Surf Coat Technol 2014;259(Part A):62–7.
[19] Wascher R, Leike N, Avramidis G, Wolkenhauer A, Militz H, Viöl W. Improved DMDHEU uptake of beech veneers after plasma treatment at atmospheric pressure. Eur J Wood Prod 2015;73:433–7.
[20] Wascher R, Avramidis G, Kühn C, Militz H, Viöl W. Plywood made from plasma-treated veneers: Shear strength after shrinkage-swelling stress. Int J Adhes Adhes 2017;78:212–5.
[21] Gindl W, Gupta HS. Cell-wall hardness and Young's modulus of melamine-modified spruce wood by nano-indentation. Composites Part A 2002;33:1141–5.
[22] Gindl W, Müller U, Teischinger A. Transverse compression strength and fracture of spruce wood modified by melamine-formaldehyde impregnation of cell walls. Wood Fiber Sci 2003;35:239–46.
[23] Gindl W, Dessipri E, Wimmer R. Using UV-microscopy to study diffusion of melamine-urea-formaldehyde resin in cell walls of spruce wood. Holzforschung 2002;56:103–7.
[24] De Vetter L, Cnudde V, Masschaele B, Jacobs PJS, Van Acker J. Detection and distribution analysis of organosilicon compounds in wood by means of SEM-EDX and micro-CT. Mater Charact 2006;56:39–48.
[25] Kamke FA, McKinley PE, Ching DJ, Zauner M, Xiao X. Micro X-ray computed tomography of adhesive bonds in wood. Wood Fiber Sci 2016;48:2–16.
[26] OWI GmbH, assignee. Verfahren zur Herstellung von witterungsbeständigem Holzfurnier sowie Holzfurnier [in German]. German Patent DE102006027934B4; 2009.
[27] Eliasson B, Kogelschatz U. Modeling and applications of silent discharge plasmas. IEEE Trans Plasma Sci 1991;19:309–23.
[28] ten Bosch L, Pfohl K, Avramidis G, Wieneke S, Viöl W, Karlovsky P. Plasma-based degradation of mycotoxins produced by Fusarium, Aspergillus and Alternaria species. Toxins 2017;9:97.
[29] Peters F, Hünnekens B, Wieneke S, Militz H, Ohms G, Viöl W. Comparison of three dielectric barrier discharges regarding their physical characteristics and influence on the adhesion properties on maple, high density fiberboards and wood plastic composite. J Phys D: Appl Phys 2017;50:475206.
[30] Wascher R, Avramidis G, Neubauer A, Seifert V, Militz H, Viöl W. Entwicklung von Vorbehandlungsmethoden für Holz und Holzwerkstoffe auf Basis einer dielektrisch behinderten Gasentladung unter Atmosphärendruck. holztechnologie 2016;57:12–7.
[31] Buzug TM. Computed Tomography: From Photon Statistics to Modern Cone-Beam CT. Berlin Heidelberg: Springer; 2008.
[32] Garcea SC, Wang Y, Withers PJ. X-ray computed tomography of polymer composites. Compos Sci Technol 2018;156:305–19.
[33] Mizutani R, Suzuki Y. X-ray microtomography in biology. Micron 2012;43:104–15.
[34] Metscher BD. MicroCT for developmental biology: a versatile tool for high-contrast 3D imaging at histological resolutions. Dev Dyn 2009;238:632–40.
[35] Pauwels E, Van Loo D, Cornillie P, Brabant L, Van Hoorebeke L. An exploratory study of contrast agents for soft tissue visualization by means of high resolution X-ray computed tomography imaging. J Microsc 2013;250:21–31.
[36] Jakes JE, Frihart CR, Hunt CG, Yelle DJ, Plaza NZ, Lorenz L, et al. X-ray methods to observe and quantify adhesive penetration into wood. J Mater Sci 2019;54:705–18.
[37] Paris JL, Kamke FA, Xiao X. X-ray computed tomography of wood-adhesive bondlines: attenuation and phase-contrast effects. Wood Sci Technol 2015;49(6):1185–208.
[38] Denaud LÉ, Bléron L, Ratle A, Marchal R. Online control of wood peeling process: acoustical and vibratory measurements of lathe checks frequency. Ann For Sci 2007;64:569–75.
[39] Veverka PJ, Horton RR, Nichols KM, Adams TN. On the form of nitrogen in wood and its fate during kraft pulping. In: Proceedings of TAPPI environmental conference. Boston, March; 1993. p. 777–80.